

# COMPUTING AN AVERAGE ANATOMICAL ATLAS USING LDDMM AND GEODESIC SHOOTING

*M. Faisal Beg and Ali Khan*

Medical Image Analysis Laboratory, School of Engineering Science, Simon Fraser University

## ABSTRACT

Average 3D digital atlas construction from a set of images is an important task for registration and assessment of intra- and inter-population differences in structural and functional imagery. In this paper, we describe the computation of an average atlas using LDDMM and geodesic shooting where the velocity vector fields transforming a provisional template to the ensemble are averaged and evolved via shooting using the equation for the geodesic conservation of momentum to give the average atlas. This guarantees that the averaged atlas so computed remains within the permissible shape space of the anatomical ensemble being averaged.

## 1. INTRODUCTION

Average 3D digital atlases [1] are important in various aspects of Computational Anatomy (CA). Typical applications of digital atlases include their use in providing a template anatomy for registration of the other members in the anatomical ensemble and establishing a standard “extrinsic” coordinate system (akin to an “origin”) for statistical analysis of structural and functional variability observed in the population. Preceding the statistical study of anatomical variation in CA, transformations that allow the placement of different members of the anatomical ensemble into a common extrinsic coordinate system are computed. The provisional template image to which the ensemble is transformed has often been chosen to be one representative member of the ensemble. However, an important feature of good atlases is that they are representative of the entire population, and include information from a set of images acquired from the population rather than being based on a single chosen proviso-template. Choosing and basing statistical analysis on the coordinates of a single image is said to introduce “bias” to this preferred common coordinates, specially in settings where the transformations are non-invertible. Therefore, averaged-atlas computation must involve the averaging of the anatomical ensemble in a meaningful way to ensure that the outcome remains representative of the topological and shape characteristics of the ensemble.

Computation of an average anatomical image is not a matter of simply averaging of the image intensities, as due to fi-

nite quantization, anatomical images do not lie in a vector space. More important is the fact that simple image averaging does not respect the “curved” manifold of the anatomical shape space. Alternatively, sufficiently rich transformations of all anatomical images to a chosen provisional template could be computed. Then, either the average of the estimated transformations could be used to transform the provisional template, or the average of vector fields (the displacement vector fields in the small-deformation, elastic matching setting or the time-indexed velocity vector fields in the large-deformation setting) parameterizing each of the estimated transformations be used to compute an average transformation of the template. Linear averaging of transformations is also not a valid operation as transformations are not a vector space. It can be done with good results in the small-deformation setting [2] where it reduces to averaging of the displacement fields. Hence, most previous approaches has focused on averaging the small deformation displacement vector fields [3, 4] or the large deformation time-indexed velocity vector fields (parameterizing diffeomorphic transformations) to compute the average [5–7]. In the context of biological images and the tremendous variability expressed in anatomical shape and form, the infinite-dimensional group  $\mathcal{G}$  of diffeomorphisms forms the natural setting in which to perform such analysis [5]. Diffeomorphisms are smooth and invertible transformations, and under their action, it is guaranteed that no fusion, folding or tearing of the anatomical imagery will be found in the transformed images.

Here, we describe the computation of an average atlas image from an ensemble of images based on the Large Deformations Diffeomorphic Metric Mapping (LDDMM) methodology [8] and the concepts of geodesic shooting in the space of diffeomorphic transformations [9]. This is an extension of the average computation in the landmark matching setting using geodesic shooting [10] where the average shape and statistical models of variability of an ensemble of landmark datasets were discussed. The average atlas in this procedure remains in the shape space of the ensemble of elements being averaged since it follows the diffeomorphic evolution of the provisional template shape via the conservation of momentum along the geodesic flow on the curved manifold of diffeomorphisms. The average atlas computation discussed here was used in quantifying variability in heart geometry [11].

## 2. REVIEW OF LDDMM

Let the background space  $\Omega \subset \mathbb{R}^n$  be a bounded domain on which the image functions in the ensemble  $\mathcal{I} = \{I : \Omega \rightarrow \mathbb{R}^d\}$  are defined. Let  $\mathcal{G}$  denote the admissible subset of the group of diffeomorphisms of the domain  $\Omega$  with the law of composition  $\psi \cdot \phi \doteq \psi \circ \phi$  (for the details related to the rigorous construction of  $\mathcal{G}$ , see [12, 13]). For any image  $I \in \mathcal{I}$ ,  $\phi I \doteq I \circ \phi^{-1}$  defines an action of  $\mathcal{G}$  on  $\mathcal{I}$ . Given a template  $I_{\text{template}}$ , an anatomical ensemble is defined as the orbit  $\mathcal{I} \doteq \{\phi I_{\text{template}} \mid \phi \in \mathcal{G}\}$  of  $I_{\text{template}}$  under the action of  $\mathcal{G}$ . Given two anatomical images  $I_0$  and  $I_1$  in the orbit, identify the first image with the identity element in  $\mathcal{G}$  and the second image with the unknown diffeomorphism  $\varphi \in \mathcal{G}$  registering the given images  $I_1 = \varphi I_0 = I_0 \circ \varphi^{-1}$ . This unknown diffeomorphism is computed as the end-point  $\varphi = \phi_1$  of a time-indexed flow  $\phi : [0, 1] \rightarrow \mathcal{G}$  associated to a smooth, compactly supported, time-dependent velocity vector field  $v_t \in V, t \in [0, 1]$  via the ODE  $\dot{\phi}_t = v_t \circ \phi_t$ , with  $\phi_0 = \text{identity}, t \in [0, 1]$ . The estimation of the optimal transformation connecting images  $I_0$  and  $I_1$  occurs via the basic variational problem that, in the Hilbert space  $V$  of smooth vector fields, takes the form:

$$\hat{v} = \underset{v: \dot{\phi}_t = v_t(\phi_t)}{\text{argmin}} \left( \int_0^1 \|v_t\|_V^2 dt + \frac{1}{\sigma^2} \|I_0 \circ \phi_1^{-1} - I_1\|_{L^2}^2 \right).$$

The optimizer  $\hat{v}$  of this cost generates, upon integration, the optimal change of coordinates  $\varphi = \phi_1$ . Enforcing a sufficient amount of smoothness via an appropriate Sobolev norm (such as through a mixture of differential operators  $L$  via  $\|f\|_V = \|Lf\|_{L^2}$ ,  $\langle f, g \rangle_V \doteq \langle Lf, Lg \rangle_{L^2}$  where  $\|\cdot\|_{L^2}$  is the standard  $L^2$  norm for square integrable functions defined on  $\Omega$ ) on the elements admissible in the space  $V$  ensures that the solution to evolution ODE is in the space of diffeomorphisms [12, 13].

The variational gradient of this variational cost function leads to the Fréchet derivative  $\nabla_v E_t$  in space  $V$  to be:

$$\nabla_v E_t = 2v_t - K \left( \frac{2}{\sigma^2} |D\phi_{t,1}| \nabla J_t^0 [J_t^0 - J_t^1] \right)$$

where the notation  $\phi_{s,t} : \Omega \rightarrow \Omega$  is used to denote the composition  $\phi_{s,t} = \phi_t \circ (\phi_s)^{-1}$ ,  $J_t^0 = I_0 \circ \phi_{t,0}$ ,  $J_t^1 = I_1 \circ \phi_{t,1}$ ,  $|D\phi_{t,1}|$ ,  $\nabla J_t^0$  are the determinant of the Jacobian and the gradient of the functions  $\phi_{t,1}$  and  $J_t^0$  respectively. The operator  $K$  is a compact self-adjoint operator such that when  $V$  is defined through a differential operator  $L$ , one gets  $K(L^\dagger L)a = a$  for any smooth vector field  $a \in V$  ( $\langle a, b \rangle_{L^2} = \langle Ka, b \rangle_V$ ) where  $L^\dagger$  is the adjoint of  $L$ . This variational gradient is used in a standard gradient based scheme exploiting the vector space structure of  $V$  yielding the update

$$v^{n+1} = v^n - \epsilon \nabla_{v^n} E$$

where  $n$  denotes the simulation number, and due to the smoothness constraints imposed on space  $V$ , enjoys nice numerical properties with respect to convergence and stability. This is

called the LDDMM solution [8] to the posed variational image matching problem as it provides (1) large deformation coordinate system transformation in the space of diffeomorphisms and (2) the length of the shortest path  $\inf \int_0^1 \|v_t\|_V dt$  connecting the given images defines a metric on the image orbit  $\mathcal{I}$  [14].

## 3. LDDMM BASED GEODESIC SHOOTING

The variational derivative vanishes on the optimizer of the variational cost. Therefore,  $\nabla_v E_t = 0$  gives that the optimal, geodesic flow satisfies:

$$\begin{aligned} (L^\dagger L)v_t &= \frac{2}{\sigma^2} |D\phi_{t,1}| \nabla J_t^0 [J_t^0 - J_t^1] \\ &= \alpha_t \nabla J_t^0 \quad \forall t \in [0, 1] \end{aligned}$$

where  $\alpha_t = (2/\sigma^2) |D\phi_{t,1}| [J_t^0 - J_t^1]$  and, at  $t = 0$ ,

$$(L^\dagger L)v_0 = \frac{2}{\sigma^2} |D\phi_{0,1}| [I_0 - I_1 \circ \phi_{0,1}] \nabla I_0 = \alpha_0 \nabla I_0.$$

The quantity  $(L^\dagger L)v_t$  is the momentum of the diffeomorphic flow at time  $t \in [0, 1]$ . A detailed and rigorous construction of the theory of geodesic shooting originates in [9]. The important property of geodesic shooting of relevance to construct the averaged atlas is that the momentum associated to the flow is conserved since  $\alpha_t = |D\phi_{t,0}| \alpha_0 \circ \phi_{t,0}$  and  $J_t^0 = (D\phi_{t,0})^t \nabla I_0 \circ \phi_{t,0}$ . This leads to the partial differential equation for conservation of momentum:

$$(L^\dagger L)v_t = |D\phi_{t,0}| (D\phi_{t,0})^t (L^\dagger L)v_0 \circ \phi_{t,0}. \quad (1)$$

which states that the momentum at time  $t \in [0, 1]$  is known given the momentum  $(L^\dagger L)v_0$  at  $t = 0$ . Therefore, the fundamental object in the setting of the solutions to large deformations template matching problems and on which to build statistical models of anatomical variability is the velocity  $v_0$  (or the momentum  $(L^\dagger L)v_0$ ). This geodesic evolution following conservation of momentum is the essence of geodesic shooting. Given either the optimal  $v_0$  or  $\alpha_0$ , the entire geodesic path for the evolution of  $I_0$  towards  $I_1$  is completely specified. If we intuitively think of  $\nabla I_0$  as being the appropriate initial ‘‘direction’’ for shooting on the manifold  $\mathcal{G}$  to reach the target  $I_1$  while traversing the geodesic, then  $\alpha_0$  is analogous to the correct ‘‘speed’’ to start off towards the target element  $\varphi = \phi_1$  on  $\mathcal{G}$ . To practically compute the geodesic evolution, if we are given say  $v_0$ , then we can compute  $\alpha_0$  from  $(L^\dagger L)v_0 = \alpha_0 \nabla I_0$  and, using semi-lagrangian integration [8],  $\phi_{t+\delta t,0}$  can also be computed, which then gives  $\alpha_{t+\delta t} = |D\phi_{t+\delta t,0}| \alpha_0 \circ \phi_{t+\delta t,0}$  and therefore the geodesic velocity vector field at the next time-step  $v_{t+\delta t}$ . Upon iteration, this computation retrieves the entire geodesic velocity vector field starting from the specification of  $I_0$  and the optimal  $v_0$ .

Hence, the first step in our approach to create an average atlas using LDDMM and geodesic shooting is to employ

LDDMM to compute the optimal transformation of a provisional template  $I_0 \in \mathcal{I}$  to each target image  $I_i \in \mathcal{I}, i = 1, \dots, N$ . The image ensemble could consist of, for example, MR images of the neuroanatomy acquired from the same scanner/pulse-sequence or segmented binary images of a given anatomical structure such as the heart etc.. These images have been preprocessed to be in rigid alignment with  $I_0$  via standard rigid registration algorithms. The set of optimal velocity vector field  $v_t^i \in V, t \in [0, 1], i = 1, \dots, N$  computed from LDDMM gives the optimal diffeomorphic change of coordinates  $\varphi^i, i = 1, \dots, N$  such that, within the noise specification in the inexact matching setting,  $\varphi^i I_0 \approx I_i$ . The second step is to compute the average initial velocity vector field at the origin  $\bar{v}_0 = (1/N) \sum_i v_0^i$ . The third step is to propagate this averaged velocity vector field  $\bar{v}_0$  forward using the conservation equation 1 stopping the evolution in the same number of discretized time-steps that were used to match each of the ensemble images to the chosen template  $I_0$ . The resultant transformation of  $I_0$  via the geodesically evolved flow is thus the computed ensemble-averaged atlas. The above procedure can be iterated with the computed average as the new template, and stopping the process when the averaged  $\|\bar{v}_0\|$  is small. The geodesic evolution guarantees that the transformation at every  $t \in [0, 1]$  is an element in the admissible group of diffeomorphisms and hence, the constructed averaged atlas adheres to the constraints of shape and topology present in the averaged ensemble.

#### 4. RESULTS

This algorithm has been implemented in C++ as a full 3D computation. The algorithm was used to calculate the population average for binary segmentations of the cardiac ventricles from normal and diseased dogs (Figure 1 a,b) and binary caudate segmentations from human MR images (Figure 2). The computed average models are found to agree with a qualitative representation of the population, and are sharp and well defined. The algorithm was also applied on grayscale MR images, a cube surrounding the basal ganglia was cut from the whole brain MR image and processed with edge preserving smoothing prior to calculating the average grayscale atlas (Figure 3). The computed atlas also shows that it is a crisp image with minimal loss of contrast and well-defined qualitatively average features. Preliminary validation of the average atlas image, in the spirit of the Fréchet mean, via  $\frac{1}{N} \sum_{i=1}^N \rho_{\mathcal{I}}^2(I_i, \bar{I})$  where  $\mathcal{I}$  is the anatomical ensemble and  $\rho_{\mathcal{I}}$  the LDDMM metric distance on  $\mathcal{I}$  indicates that this procedure leads to a lower sum of the squared distances from the computed average atlas image.

#### 5. CONCLUSION

This paper presents an algorithm for computing a digital 3D anatomical average atlas from an ensemble of images using

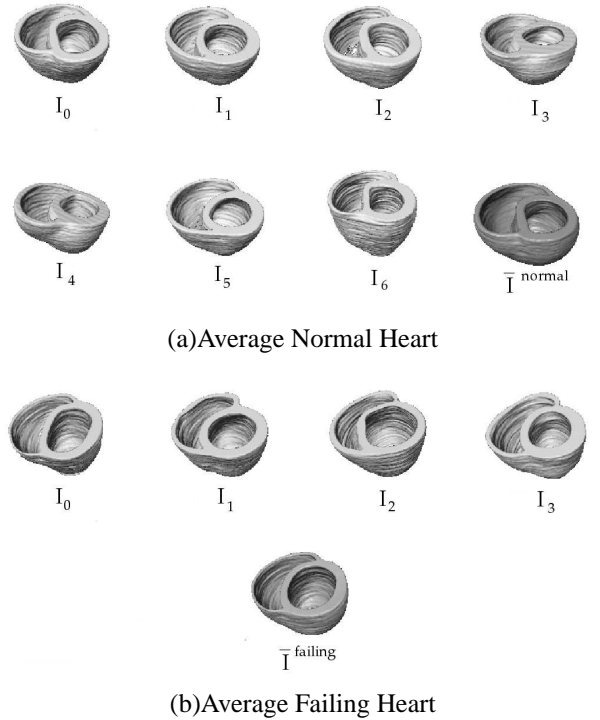
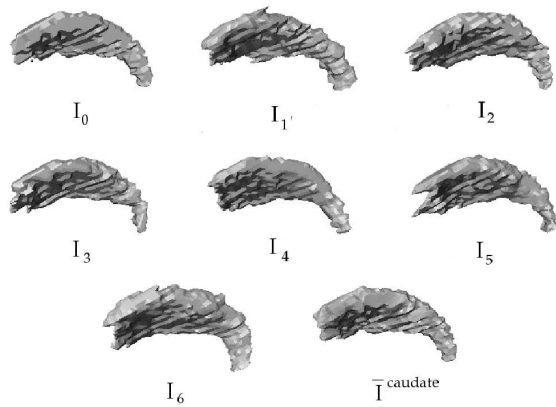


**Fig. 1.** Segmented binary models of the normal and diseased dog hearts were used to compute the respective population average model  $\bar{I}^{normal}$  and  $\bar{I}^{failing}$ .

LDDMM and geodesic shooting. The computations are stable and fast, and the computed atlas has image quality and contrast similar to the ensemble with minimal blurring effects entering due to interpolation upon transformation and not inherent to the averaging procedure. This is due to the averaging of geodesic velocity vector fields in the coordinates of a chosen template and their evolution on the manifold of diffeomorphisms via geodesic shooting, thus always ensuring that the computed average image remains within the orbit of template under diffeomorphisms. As a result, the computed average is also found to preserve the topology of the template and represent the average of the variability manifest in the population.

#### 6. ACKNOWLEDGEMENTS

The heart data was provided by Dr. Patrick Helm at the Center for Computational Biology and Medicine at JHU, the caudate datasets were courtesy of Professor Elizabeth Aylward at the University of Washington, Department of Radiology. This work was supported by Natural Sciences and Engineering Research Council of Canada Discovery Grant 31-611387 and HighQ foundation grant 31-579043.

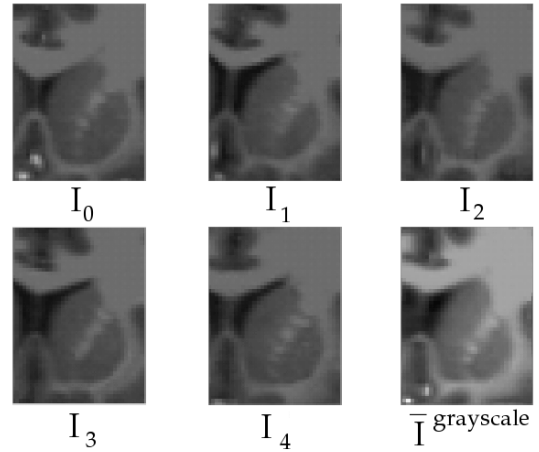


Average Segmented Caudate

**Fig. 2.** Segmented binary models of the caudate were used to compute the respective population average model  $\bar{I}^{caudate}$ .

## 7. REFERENCES

- [1] P. M. Thompson, R. P. Woods, M. S. Mega, and A. W. Toga, "Mathematical/computational challenges in creating deformable and probabilistic atlases of the human brain," *Human Brain Mapping*, vol. 9, no. 2, pp. 81–92, 2000.
- [2] G. E. Christensen, H. J. Johnson, J. W. Haller, J. Melloy, M. W. Vannier, and J. L. Marsh, "Synthesizing average 3d anatomical shapes using deformable templates," 1999, vol. 3661, pp. 574–582, SPIE.
- [3] A. Guimond, J. Meunier, and J.-P. Thirion, "Average brain models: A convergence study," *Computer Vision and Image Understanding*, vol. 77, no. 2, pp. 192–210, 2000.
- [4] K. Bhatia, J. Hajnal, B. Puri, A. Edwards, and D. Rueckert, "Consistent groupwise non-rigid registration for atlas construction," 2004, pp. 908–911, ISBI.
- [5] U. Grenander and M. I. Miller, "Computational anatomy: An emerging discipline," *Quarterly of Applied Mathematics*, vol. 56, pp. 617–694, 1998.
- [6] B. Avants and J. C. Gee, "Geodesic estimation for large deformation anatomical shape averaging and interpolation," 2004, vol. 23, pp. S139–S150, NeuroImage.
- [7] P. Lorenzen, B. Davis, and S. Joshi, "Unbiased atlas formation via large deformations metric mapping," 2005, pp. 411–418, MICCAI.
- [8] M. F. Beg, M. Miller, A. Trouvé, and L. Younes, "Computing metrics via geodesics on flows of diffeomorphisms," *International Journal of Computer Vision*, vol. 61, no. 2, pp. 139–157, February 2005.
- [9] M. Miller, A. Trouvé, and L. Younes, "Geodesic shooting for computational anatomy," *Journal of Mathematical Imaging and Vision*, Jan 2006.
- [10] M. Vaillant, M.I. Miller, L. Younes, and A. Trouvé, "Statistics on diffeomorphisms via tangent space representations," *NeuroImage*, vol. 23, no. 1, pp. S161–S169, 2004.
- [11] P. Helm, L. Younes, M. F. Beg, D. Ennis, C. Leclercq, O. Faris, E. McVeigh, M.I. Miller, and R. Winslow, "Evidence of structural remodeling in the dyssynchronous failing heart," *Circulation Research*, pp. 98–125, 2006.
- [12] P. Dupuis, U. Grenander, and M.I. Miller, "Variational problems on flows of diffeomorphisms for image matching," *Quarterly of Applied Mathematics*, vol. LVI, pp. 587–600, September 1998.
- [13] A. Trouvé, "An infinite dimensional group approach for physics based models in patterns recognition," *Preprint*, 1995.
- [14] M.I. Miller and L. Younes, "Group actions, homeomorphisms, and matching: a general framework," *International Journal of Computer Vision*, vol. 41, pp. 61–84, 2001.



Average grayscale MRI image

**Fig. 3.** Grayscale MR image cube cut around the basal ganglia from different individuals' MR images were used to compute the respective population average model  $\bar{I}^{grayscale}$ . Shown are corresponding 2D sections from the 3D population images and the computed average. Note the well-defined anatomical features preserved in the average grayscale image.